Author's response to:
RC#2
https://doi.org/10.5194/egusphere-2025-4517-RC2

Anton Kötsche[1], Maximilian Maahn[1], Veronika Ettrichrätz[1], and Heike Kalesse-Los[1]
[1]Leipzig Institute for Meteorology (LIM), Leipzig University, Leipzig, Germany
Correspondence: anton.koetsche@uni-leipzig.de

Dear Reviewer,

Thank you for carefully reading the manuscript and pointing out several issues where the description needs to be refined for a better understanding. The requested clarifications and references to ambiguities contribute to the improvement of the manuscript.

To separate the Reviewer's comments and the author's response, we printed the comments in black and the response in blue. Excerpts of the manuscript with marked changes are pinned directly to the appropriate responses, with the indicated text location (e.g., line number) referring to the manuscript in the preprint.

Sincerely, on behalf of all authors

Anton Kötsche

Summary of main changes of the manuscript:

- There was a minor bug in the processing of the turbulent layer height. The EDR data was re-gridded to fit the range resolution of the ARM wind profiles, effectively halving the range resolution of EDR. This EDR was then used to process TLH, TLH was then used for all statistics presented in the manuscript. Of course, this was not necessary for most of the statistics where EDR could have been kept at full resolution. We addressed that issue and reprocessed all statistics, the overall impact however was minimal.
- Some minor changes occured in Fig. 9, there was a bug in the statistic where some of the "no turbulence" cases were falsely classified.
- A paragraph was added in L.168f. explaining the reasons for the used turbulent layer height retrieval
- As suggested by both reviewers, we created a schematic figure of main suspected processes in the turbulent layer (see Fig. 6) and added it to Sec. 3.3.
- A map of the measurement sites topography was added in the appendix of the manuscript (see Fig. B1). We also referenced the figure in Sect. 3.2.
- We removed backscattering differential phase cases from the statistics presented in Sect. 3.3 because it falsely affected overall K_{DP} magnitude. In the statistic presented in Fig. 11, minor changes in ΔK_{DP} occured. Details on how backscattering differential phase were provided in Sect. 2.1.2.
- In cases with shallow precipitating clouds, when their cloud top and the turbulent layer are superimposed, primary nucleation may be especially active and we can not exclude the impact of ice nucleation on our statistic. These cases almost never end up in the statistic because no data will be present above the turbulent layer. The few cases that would have been included in the statistic were removed. Additional argumentation was added in Sect. 2.7.

Response to RC#2:

I am very skeptical on the interpretation of shallow precipitation cases where the turbulent layer almost overlays with cloud top. Since you want to get snow microphysical signatures, your basic assumption is that the turbulence affects snow growth and ice nucleation should play a minor role. However, the turbulent layer is so close to the cloud top where ice nucleation is actively taking place that you cannot exclude the impact of ice nucleation. In this regard, you are not comparing snow before and after entering the turbulent layer. You may check Chellini, G. and Kneifel 2024, and see how you can disentangle the impact of turbulence. I would suggest remove shallow precipitation cases. You may discuss how turbulence affects snow FORMATION in a separate study, but not here.

Thank you for pointing out this very important issue with our analysis. We are aware of the general impact of INP and nucleation in the turbulent layer, however, we assume this effect to be comparably small for two reasons. The first is that the shallow precipitation cases almost never end up in the statistic presented in the main Figure 11 (28 out of 1925 time stamps used in the analysis). The reason is that when comparing data above and below the turbulent layer, no data will be present above the turbulent layer if the turbulent layer is near the cloud top. For identifying shallow precipitation cases we used the same criteria as in Figure 9 of the manuscript. We removed the shallow cases from the statistics. The second reason is related to the number of INPs present at the site. A very recent study (preprint) on the INP concentration during SAIL revealed that INP number concentrations are indeed very low in the temperature region we are interested in. Please see Figure 5 in Zhou et al. (2025), we also took a screenshot of this figure and included it here for you to look at (see Fig. 1). At temperatures around -15 °C or warmer, the INP concentration is $10^{-2}\,\mathrm{L}^{-1}$ or lower. We included this argumentation in the paper draft so improve out argumentation.

L218f.:

We are furthermore aware that ice nucleation through ice nucleating particles (INP) may constantly occur inside the turbulent layer in parallel to SIP and thereby adulterate the analysis. However, a recent study of Zhou et al. (2025) on the INP concentrations during the SAIL campaign found the INP concentrations during the cold season to be $10^{-2}\,\mathrm{L}^{-1}$ or less at temperatures of -15 °C or warmer, which is the primary temperature region we find the turbulent layer in during our analysis. Therefore, the impact of primary ice nucleation on the total number concentration can assumed to be small. In case of precipitation from a shallow cloud layer, where the turbulent layer is close to the cloud top, the effect of primary ice nucleation may be more significant. However, these cases almost never end up in the statistic because no data will be present above the turbulent layer. The few cases that would have been included in the statistic were removed. These cases were identified using KAZR Z_e, the criterion for precipitation from a shallow cloud layer was fulfilled if KAZR Z_e between 500 m and 1.5 km above Gothic Mountain summit height did not exceed -10 dBZ.

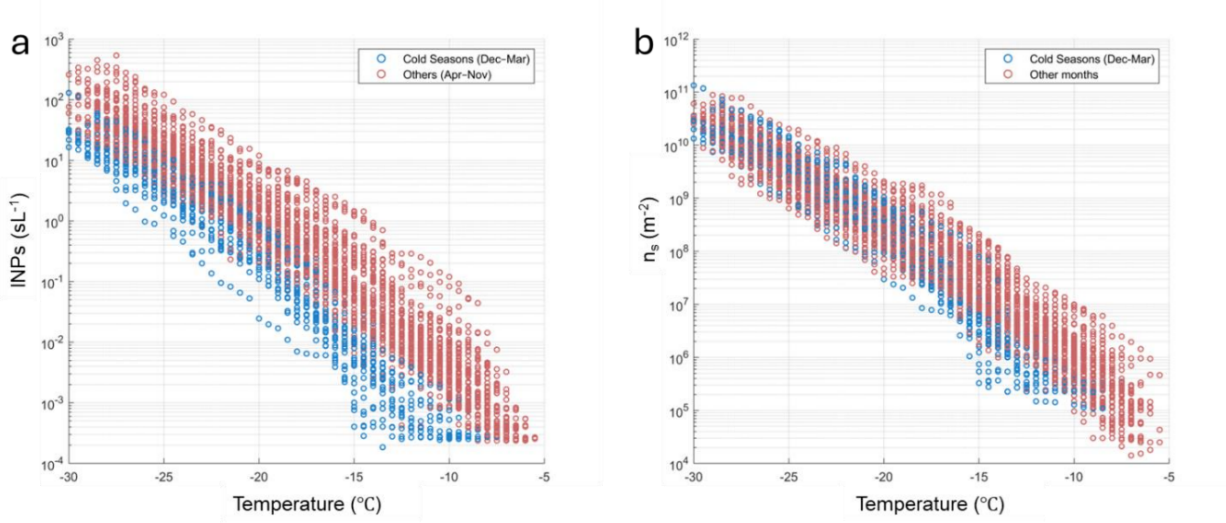

Figure 5. (a) INP temperature spectra and (b) IN active surface site density (n_s) categorized by sampling date as cold seasons (December–March) and other seasons (April–November). n_s was calculated based on the surface area of particles larger than 500 nm.

Figure 1. Screenshot of Figure 5 from Zhou et al. (2025)

Comments

- *L108 How did you compute KDP from PHIDP? At W-band, you may expect non-Rayleigh scattering. How did you deal with the contamination of differential backscatter phase shift?*

- Thank you for pointing out this important point, first of all, K_{DP} was calculated from Φ_{DP} using a convolution with low-noise Lanczos differentiators with window length of 23 gates. This method provides results that are analogue to a moving window linear regression and is implemented in the python package wradlib (Heistermann et al., 2013). Backscattering differential phase δ is an important issue with our analysis. We usually see δ associated with larger graupel, occurring comparably seldom in our dataset. Due to noise in PhiDP and the comparably small number of range gates (i.e. smoothing) we applied to calculate K_{DP}, we may see slightly negative K_{DP}, especially along cloud edges, which is mostly related to non-uniform beam filling rather than δ. Due to the temporal averaging we apply to the data, we assumed δ to be negligible at first, but based on your comment we had a closer look and detected the occurrence of δ using K_{DP} and Z_e thresholds. We defined δ to be present where K_{DP} is below -0.5 $°km^{-1}$, Z_e is higher than 0 dBZ and SNR is above 10 dB. We then removed all profiles where more than 10 range gates fulfilled the backscatter criterion. This means we are not just masking negative K_{DP}, we also remove positive K_{DP} that may result of bumps in PhiDP

caused by non-Rayleigh effects. The reprocessed statistic is shown in Fig. 2. As expected, a few cases with graupel were removed, the overall change is rather small. Mostly, there is a slight increase in K_{DP} in quadrant II, presumably because negative K_{DP} causes by back scatter was removed. Please not that in that version of the figure, the shallow precipitation cases were also removed already. We added a section on δ in Sect 2.1.2:

L108f.:

The differential phase shift $\Phi_{DP}\,(^\circ)$ consists of a backscatter and a propagational part, where the propagational part is called specific differential phase $K_{DP}\,(^\circ\,\mathrm{km}^{-1})$. We calculated K_{DP} from Φ_{DP} using a convolution with low-noise Lanczos differentiators with a window length of 23 gates. This method is implemented in the python package wradlib (Heistermann et al., 2013). Backscatter differential phase (δ) is caused by hydrometeors large enough relative to the radar wavelength such that the scattering is in the non-Rayleigh regime (Trömel et al., 2013). δ was found to be negligible for frozen hydrometeors in the S, C, and X-bands (Balakrishnan and Zrnic, 1990; Ryzhkov et al., 2011; Trömel et al., 2013). In the data of our W-band radar however, we find a contribution of δ, predominantly during cases with large graupel. Because removing the δ contribution from Φ_{DP} is not easy to perform, we chose to omit radar data where δ is occurring. δ causes so called bumps, sudden increases in Φ_{DP} followed by a decrease. This results in negative K_{DP} values, which are therefore a good indicator for δ. We defined δ to be present if K_{DP} in a radar range gate is below -0.5 $^\circ km^{-1}$, Z_e is higher than 0 dBZ and SNR is above 10 dB. We then removed all profiles where more than 10 range gates fulfilled the δ criterion.

– *L117. Check the definition of ZDR. It is undoubtedly affected by particle concentration. I would simply remove this sentence.*

– We agree that the sentence might be misleading. Z_{DR} is defined as follows:

$$Z_{DR} = 10 \cdot \log_{10}\left(\frac{Ze_H}{Ze_V}\right) \tag{1}$$

where both Z_H and Z_V are proportional to the number of particles, correct. But when number concentration is increased, both Z_H and Z_V increase by the same factor, so their ratio and hence Z_{DR} stays the same. Z_{DR} is therefore unaffected by the particle concentration. But of course, a certain number of particles must be present to produce Z_e in the first place. To clarify, we replaced the sentence by a more precise wording:

L128f.:

Unlike K_{DP}, Z_{DR} is ~~unaffected by the particle concentration .~~ immune to the total concentration factor.

– *L121. Not really true. Firstly, overall ZDR is not affected by spectral broadening. Then, speaking of the spectral analysis, spectral broadening may lead to smaller maximum spectral ZDR, but is not necessarily lowering all spectral ZDR.Regarding the impact of turbulence on ZDR, I believe you are referring to more scattered canting angles in enhanced turbulence. See literature below,*

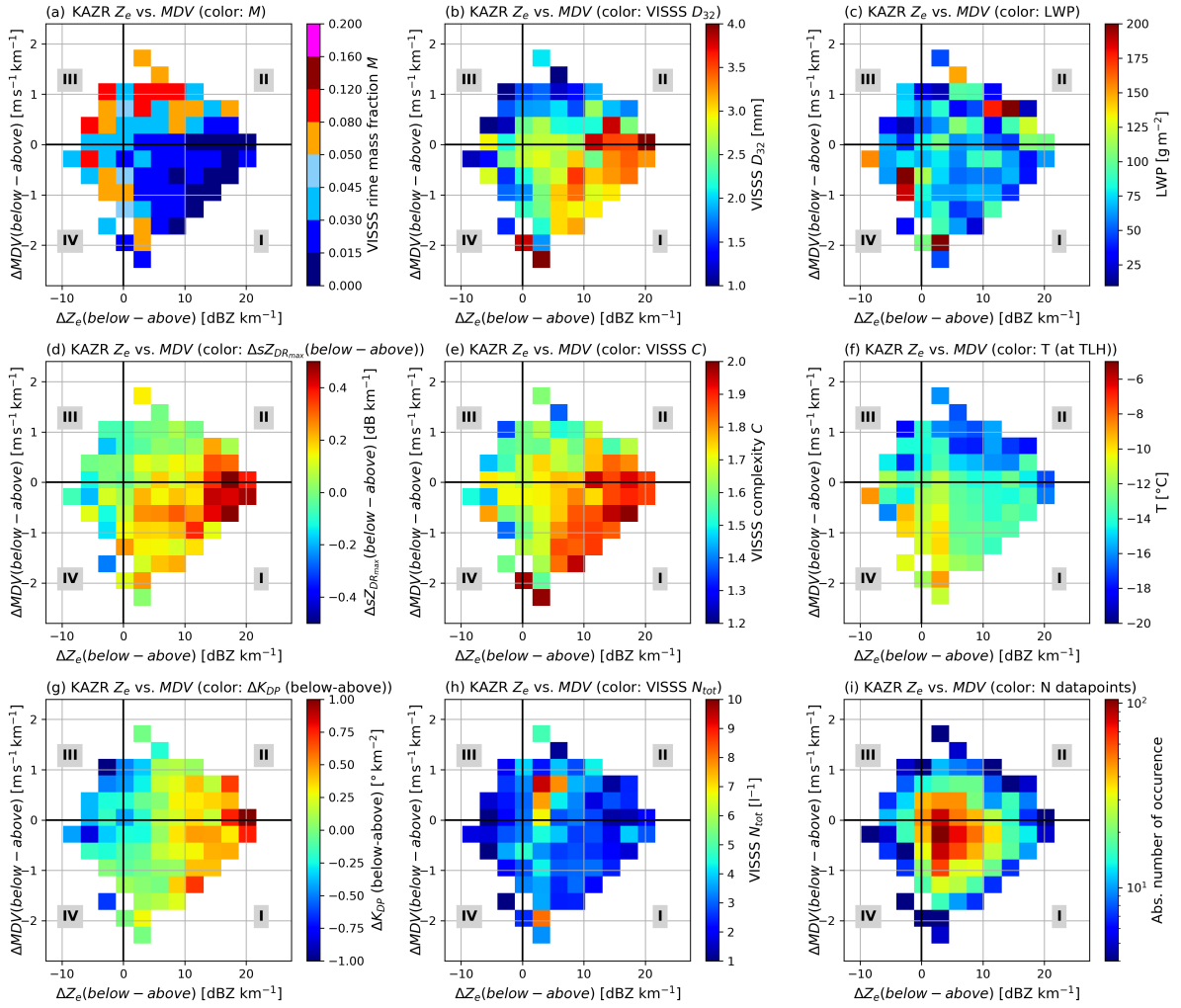

Figure 2. Updated Figure 11, backscattering differential phase cases and shallow precipitation cases removed.

– You are correct, ZDR is not affected by spectral broadening, and by more random orentation of particles we mean the width of the canting angle distribution as stated above when describing K_{DP}. We adapted the sentence to be more precise:

> **L132f.**:
>
> Similar to K_{DP}, overall Z_{DR} values are reduced by turbulence through ~~a more random orientation of particles and~~ an increased width of the canting angle distribution. $sZ_{DR_{max}}$ is furthermore reduced by broadening of the Doppler spectrum caused by turbulence.

– *L134 What is VAP?*

– This means value added product, we replaced VAP with "value added product" in the text.

– *L136 How did you merge sonding and MWR data?*

– This VAP is produced by ARM and we do not take part in the processing, however we did state that MWR temperature data is included in the retrieval. Actually, only precipitable water vapor from the MWR data is included.

L150f.:

~~The sounding data ,~~ For the processing, ARM uses sounding data collected on site through two radiosonde launches per day (11 and 23 UTC)~~, is transformed~~ . They then transform the data into continuous daily files with 1-minute time resolution and combined with ARM 3-channel microwave radiometer ~~temperature~~ precipitable water vapor data.

– *L146 In ARCTRIS framework, turbulence is estimated with O'Connor et al., 2010. What is the difference between the two approaches? Did you get consistent results from Vogl et al., 2024?*

– The two methods retrieve turbulence in different ways: O'Connor et al. (2010) estimate EDR from the short-time variance of successive mean Doppler-velocity measurements (a direct variance method), whereas Vogl et al. (2024) derive EDR from the -5/3 inertial-range slope of the mean-Doppler-velocity power spectrum over multi-minute windows (a spectral-slope method). Thus, O'Connor uses small-scale, high-frequency fluctuations, while Vogl relies on identifying an inertial subrange in the MDV spectrum. As we did not apply the retrieval of O'Connor et al. (2010) and therefore cannot comment on how consistent both results are.

– *L207 Time-height plot of EDR should be given, so that the reviewer is convinced that the EDR retrieval and turbulence layer classification are reasonable.*

– Please see Fig. 3 (b).

– *L222 I do not see evidence of sublimation from Z. A quantitative comparison is needed.*

– Please see Fig. 4 for a quantitative comparison of Ze evolution during the case study.

– *L231 It is common to see velocity oscillations at cloud tops. Why did you attribute the formation of the turbulence layer to the mountain effect?*

– Thank you for this important question, and you are right, it is of course not trivial to directly attribute the impact of Gothic Mountain on the turbulent layer. We can only assume a link to orography because of circumstantial evidence:

1. Immediate upstream proximity of Gothic Mountain, less than 2km between summit and measurement volume.
2. Collocation between turbulent layer and summit height.

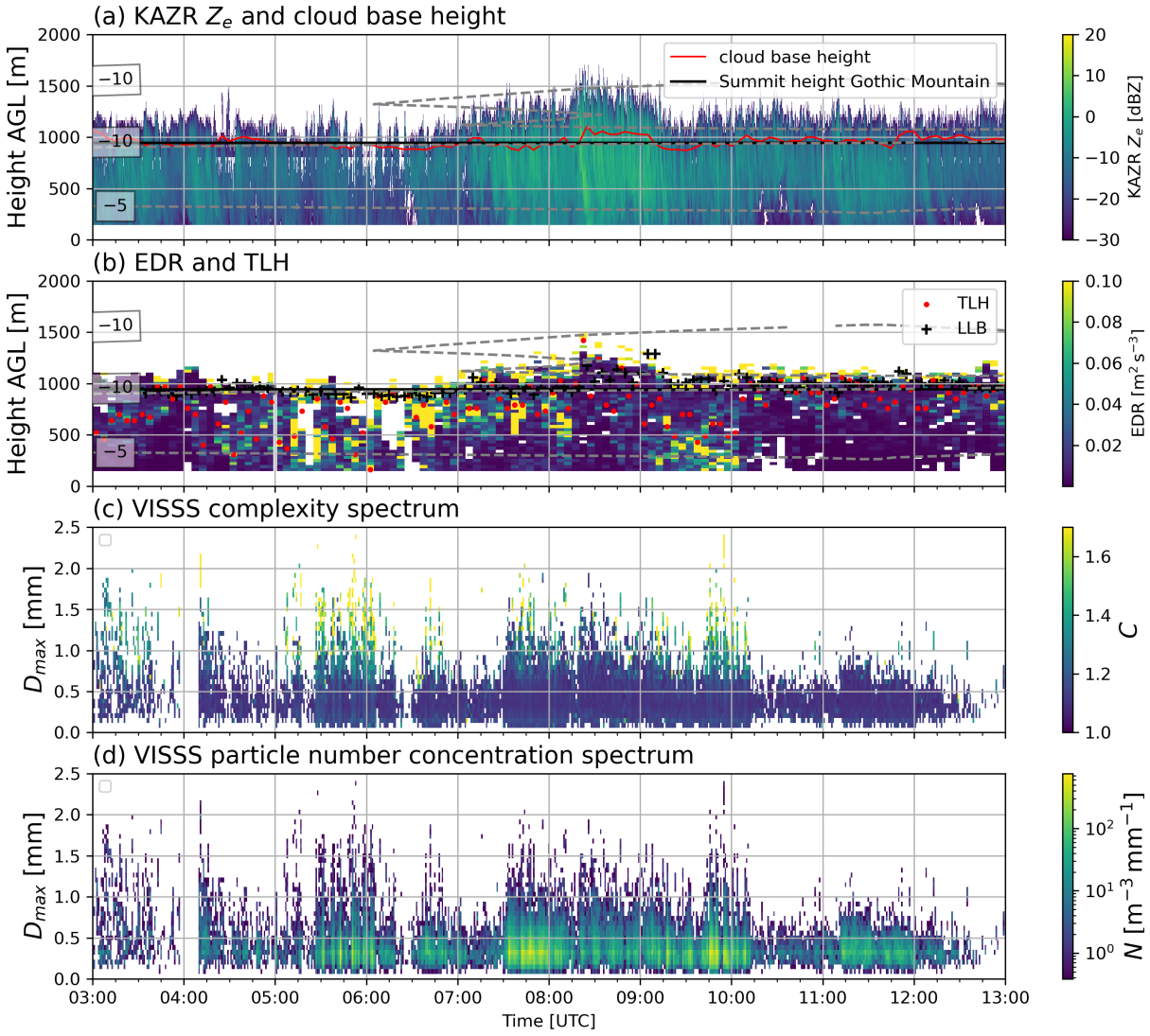

Figure 3. Casestudy panel for 21.02.2023 with EDR plotted in panel (b)

3. Wind speed increase above Gothic mountain summit height (may also be caused because of the position of the inversion, however the inversion may have been strengthened by the turbulent mixing of the atmosphere below it. This is hard to disentangle).
4. Statistical evidence of the collocation between Gothic Mountain summit height and turbulent layer height depending on the wind direction.

– *L234. This is not a good case showing the impact of turbulence. Ideally, you may show that the turbulent layer is located in the ice growth path. However, cloud top is in the turbulent layer in this case.*

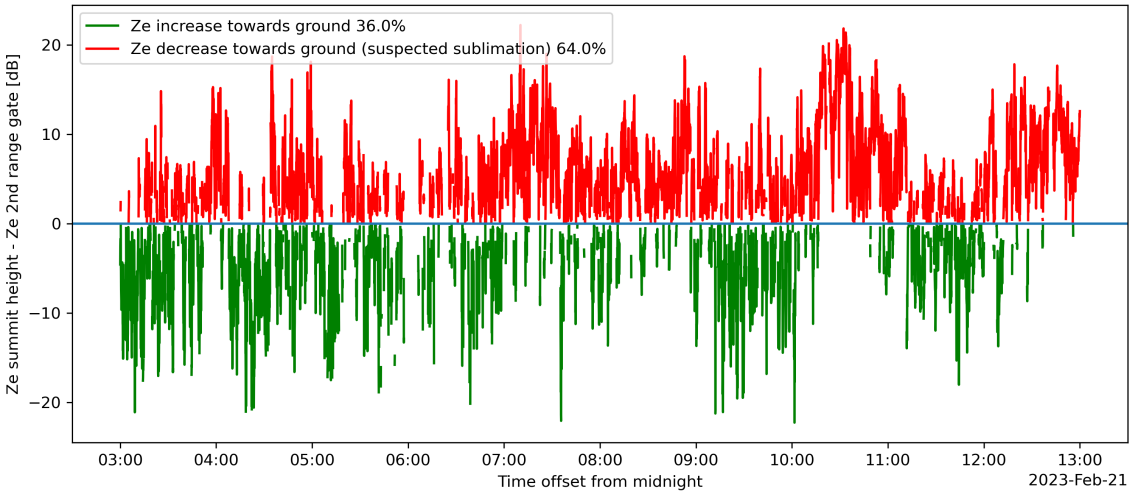

Figure 4. KAZR Ze difference between Gothic Mountain summit height and 2nd range gate above ground.

- *L238. Again, there is a critical inference issue for shallow precipitation cases. The turbulent layer almost overlays the cloud top, and ice nucleation processes are actively taking place in the turbulent layer. Then, when you are inferring ice growth processes by comparing the observations above and below the turbulent layer, you cannot rule out the role of ice nucleation and rapid deposition in local updrafts.The nice part of Chellini and Kneifel (2024) is that the turbulent layer is well below the cloud top, and the impact of ice nucleation is minimized.*

- In our opinion, especially this shallow precipitation case reveals the importance of the turbulent layer. There is no seeding particles from above, which means all the microphysics occur inside the shallow cloud layer influenced by turbulence. Temperatures inside the clouds are not cooler than -12 °C, which translates to max. 3e-3 INP per Liter (3 per m^{-3}) looking at Fig. 1 blue dots. We now use this number as max. possible particle number through INP activation, see Fig 5. We see that Ntot during the case study even during times with weak precipitation is still 1 - 3 orders of magnitude larger than what would be possible through INP activation alone. This shows SIP is likely responsible for the remaining majority of detected particles.

- *L295 Because of the concern given above, I am afraid that interpretating statistics in Fig. 10 is not well supported.*

- As mentioned above, shallow precipitation cases almost never end up in the statistic and the remaining ones were removed. The statistic remained almost unaffected by this.

- *Fig 11. Some obvious issues.Full physical meaning of the abbreviations should be given.(a) (c). High riming should fall in high LWP regions. However, the inverse is presented.(d) (g). Hight KDP and ZDRmax can simply a result of depositional growth in the turbulent layer, instead of secondary ice. A conceptual diagram should be given.*

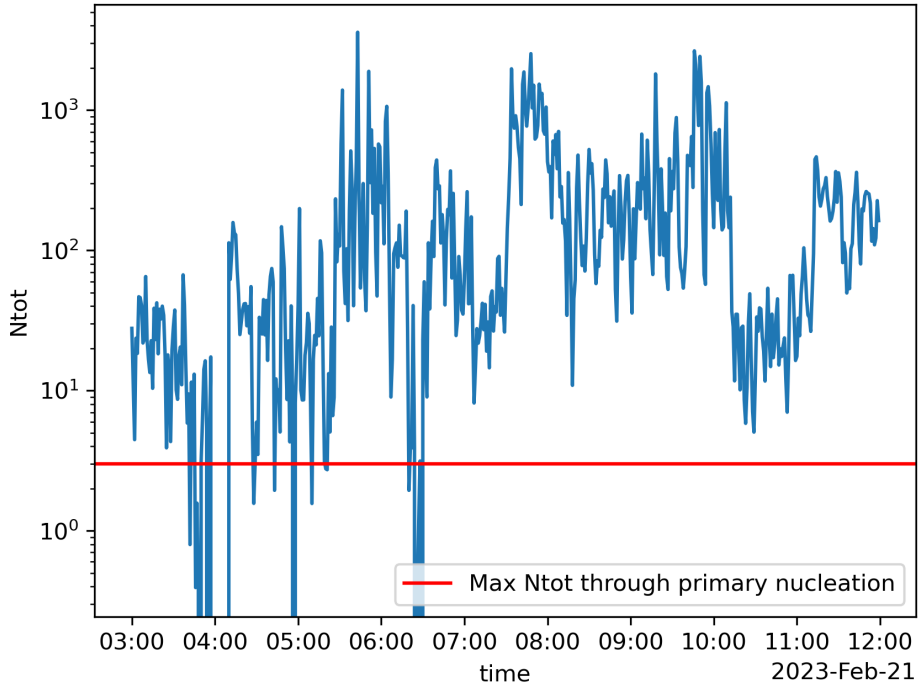

Figure 5. VISSS Ntot [m^{-3}] and max. Ntot through INP activation for case study on Feb. 21 2023

– (a) Due to limited space in the Fig, not all variables can be depicted with full name, we added the full name on the colorbar if possible. (c) The signal got a bit clearer now, however high LWP is not necessary present during riming at this site. Especially if the liquid water is produced by the turbulent layer, there is no large LWP signal but still we see increased riming. (g) yes, we agree that KDP and sZDRmax are increased by depositional growth, this is one of our arguments. However, we argue that the majority of pristine crystals originates from ice splinters produced through SIP which serve as ice embryos. Given the low INP number, we assume SIP to be the driving factor here. One graupel-snowflake collision produces up to 500 fragments per collision Grzegorczyk et al. (2023). One of these collisions per cubic meter would provide more embryos for depositional growth than 166 m^3 of air containing the max. number of INP found by Zhou et al. (2025).

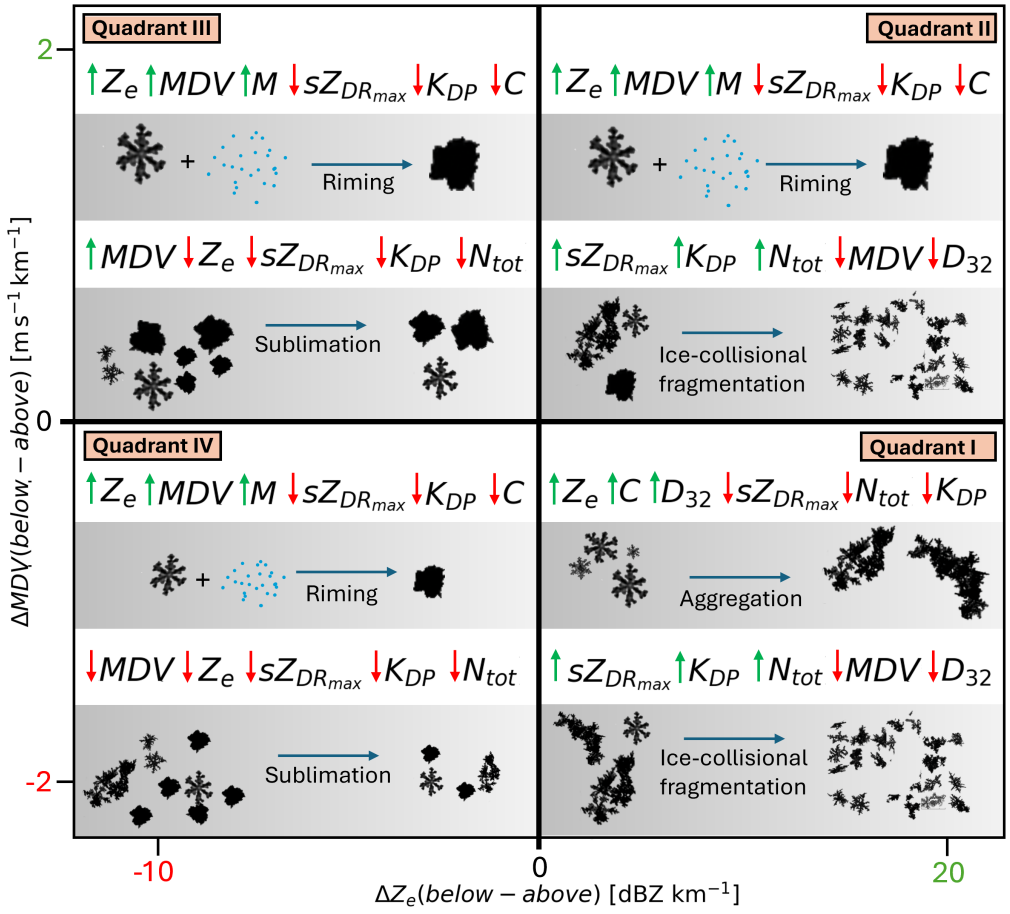

Figure 6. Conceptual diagram of the suspected (dominant) microphysical processes inside the turbulent layer, displayed similar to the four quadrants in Fig. 11. The impact of microphysical processes on radar and VISSS variables is also displayed qualitatively: Red downward facing arrows indicate a decrease of the respective variable, upward facing green arrows an increase. Note that for the radar variables (Z_e, MDV, $sZ_{DR_{max}}$ and K_{DP}), we can measure the change inside the turbulent layer. VISSS variables (N_{tot}, C, D_{32}, M) are measured below the turbulent layer. Their change due to the microphysical process is suspected based on the change of particle and PSD properties. If a variable is not depicted, no clear trend can be derived. The particle images were recorded by VISSS.

References

Balakrishnan, N. and Zrnic, D. S.: Use of polarization to characterize precipitation and discriminate large hail, Journal of the Atmospheric Sciences, 47, 1525–1540, http://ams.allenpress.com/perlserv/?request=get-abstract&doi=10.1175%2F1520-0469(1990)047%3C1525:UOPTCP%3E2.0.CO%3B2, number: 13 Publisher: American Meteorological Society, 1990.

Grzegorczyk, P., Yadav, S., Zanger, F., Theis, A., Mitra, S. K., Borrmann, S., and Szakáll, M.: Fragmentation of ice particles: laboratory experiments on graupel–graupel and graupel–snowflake collisions, Atmospheric Chemistry and Physics, 23, 13 505–13 521, https://acp.copernicus.org/articles/23/13505/2023/, publisher: Copernicus Publications Göttingen, Germany, 2023.

Heistermann, M., Jacobi, S., and Pfaff, T.: An open source library for processing weather radar data (wradlib), Hydrology and Earth System Sciences, 17, 863–871, https://hess.copernicus.org/articles/17/863/2013/, publisher: Copernicus Publications Göttingen, Germany, 2013.

Ryzhkov, A., Pinsky, M., Pokrovsky, A., and Khain, A.: Polarimetric Radar Observation Operator for a Cloud Model with Spectral Microphysics, https://doi.org/10.1175/2010JAMC2363.1, section: Journal of Applied Meteorology and Climatology, 2011.

Trömel, S., Kumjian, M. R., Ryzhkov, A. V., Simmer, C., and Diederich, M.: Backscatter Differential Phase—Estimation and Variability, https://doi.org/10.1175/JAMC-D-13-0124.1, section: Journal of Applied Meteorology and Climatology, 2013.

Zhou, R., Perkins, R., Juergensen, D., Barry, K., Ayars, K., Dutton, O., DeMott, P., and Kreidenweis, S.: Seasonal variability, sources, and parameterization of ice-nucleating particles in the Rocky Mountain region, EGUsphere, pp. 1–48, https://doi.org/10.5194/egusphere-2025-4306, publisher: Copernicus GmbH, 2025.